SPE/ISRM 78174

Deformation Analysis in Reservoir Space (DARS): A Simple Formalism for Prediction of Reservoir Deformation With Depletion

A.W. Chan and M.D. Zoback, SPE, Dept. of Geophysics, Stanford University

This paper was prepared for presentation at the SPE/ISRM Rock Mechanics Conference held in Irving, Texas, 20-23 October 2002.

Abstract

We introduce a formalism, Deformation Analysis in Reservoir Space (DARS), to quantitatively predict the degree of compaction and potential for induced faulting in a depleting reservoir. Compaction occurs when the stress state exceeds the end cap (or critical state) of a formation at any given porosity. For reservoirs in which the vertical stress is larger than the two horizontal stresses, there is also a potential to induce normal faulting in a depleting reservoir when the change of minimum horizontal stress, ΔS_h, exceeds a critical fraction of ΔP_p (the change in formation pressure due to depletion). The stress path defines the change in horizontal stress with depletion ($\boldsymbol{A}=\Delta S_h/\Delta P_p$). Utilizing relatively simple laboratory experiments, we transform the end caps from laboratory space into reservoir space (DARS) such that production data can be evaluated directly to study the evolution of the deforming reservoir due to production. Field X in the Gulf of Mexico is examined in the context of the DARS analysis. The analysis shows that the initial state of the reservoir was such that normal faults present in the field were active. However, production-induced normal faulting is not likely to occur. Deformation is dominated by compaction. Our analysis estimates that porosity of the formation was reduced from about 23% to 21%, while the permeability was reduced from about 230md to 50-140md.

Introduction

The deformation mechanisms operative in a depleting reservoir are important to understand for a variety of reasons. While it is well known that depletion can induce marked reductions in porosity (leading to compaction and possibly subsidence), it is desirable to predict the degree of compaction that might accompany depletion, the possible degree of permeability loss and, in some fields, the possibility that production-induced faulting might occur.

In this study we describe a formalism by which it is possible to integrate relatively simple laboratory rock deformation data with the physical state of a reservoir to predict its evolution through time. We refer to this as Deformation Analysis in Reservoir Space (DARS) because it attempts to quantitatively "map", through time, the nature of the deformation fields inferred from laboratory experiments into the parametric space that defines the mechanical state of a reservoir (that is, the *in-situ* principal stresses and pore pressure).

In the sections below we first provide the theoretical framework for this analysis and then consider a case study in which both laboratory and field data are available that allow us to evaluate the quantitative effects of depletion.

One important component of this analysis is the change in horizontal stress, ΔS_h, that accompanies a given amount of depletion, ΔP_P, termed the stress path, $\boldsymbol{A}$. Poroelastic theory is often used for predicting the changes in magnitude of stresses with depletion. For an isotropic, porous and elastic reservoir that is laterally extensive with respect to its thickness (20:1), the following is applicable[1].

$$\frac{\Delta S_h}{\Delta P_P} = \alpha \frac{1-2\nu}{1-\nu} \text{ and } \Delta S_V = 0 \quad \text{..... (1)}$$

where ν is Poisson's ratio and α is the Biot coefficient, $\alpha = 1 - K_b/K_g$, where K_b is the bulk modulus of the bulk rock and K_g is the bulk modulus of the mineral grains. Figure 1 demonstrates how the Biot coefficient, α, and Poisson's ratio, ν, affect the stress path. In practice, however, a depleting reservoir can undergo both elastic and significant inelastic deformation during depletion. Published data on minimum horizontal stress changes with depletion are very limited, the field names on the right hand side of Figure 1 are some published values of observed stress paths. Unfortunately, some of these reported values may not be directly related to depletion (*italic* and marked unknown) but a combination of all stress and pore pressure measurements in the field. Without

knowing the values of α or ν, it is still possible to identify if induced normal faulting will occur in these selected fields.

As pointed out by Zoback and Zinke[2], in a normal faulting stress environment (in which the vertical stress, S_v is larger than the two horizontal stresses, S_{Hmax} and S_{hmin}), the reduction of the least principal stress with depletion can induce normal faulting within a reservoir if the stress path exceeds 0.67. The horizontal straight line in Figure 1 labeled "normal faulting" corresponds to the Coulomb failure condition for normal faulting based on[3]:

$$\frac{(S_V - P_p)}{(S_{h\min} - P_p)} = \left(\sqrt{\mu^2 + 1} + \mu\right)^2 \quad \text{..... (2)}$$

We utilize coefficients of friction of μ = 0.6, which is frequently measured in the laboratory for a wide variety of rocks[4] and confirmed by in situ stress measurements[5,6]. In this case, when μ = 0.6, the stress path at which depletion will eventually lead to normal faulting is about 0.67.

The evolution of stress and pore pressure for a depleting reservoir with a steep stress path can induce normal faulting even if the initial stress state in the formation is not close to shear failure[2]. In fact, anytime ***A*** is larger than ~ 0.67, the stress path will eventually intersect the normal faulting failure line. In contrast, if ***A*** is smaller than 0.67, the potential of production-induced normal faulting decreases with production (this will be illustrated below). Note that about half of the fields in Figure 1 have an "unstable" stress path implying the potential for production-induced normal faulting. Moreover, some of the stress paths are so high that one must question the applicability of poroelastic theory, because of the likelihood of inelastic deformation. Thus, it is always preferable to determine directly the stress path a reservoir is following, rather than assume poroelastic theory is applicable, although this may be perfectly appropriate in some cases.

Shear Enhanced Compaction and Production-Induced Normal Faulting

When reservoir rock is subjected to compressive loading, the formation materials will pass through progressive states of deformation when the in-situ stress exceeds a material's failure limits. These limits are quantitative parameters that can be obtained from laboratory experiments. For example, in hydrostatic compression tests, it is straightforward to measure porosity loss with confining pressure. In triaxial tests, the compressive or frictional strength of a given sample can be straightforwardly determined. However, in actual reservoirs (i.e., in "reservoir space'), the *in-situ* stress state is anisotropic and it is not always clear how to translate laboratory-derived deformation tests into a prediction of mechanical response of a formation.

To address this problem, a theoretical formalism known as a 'Cam-Clay' model[7] is used for describing laboratory deformation data. In this case, the failure envelopes are determined by relatively simple laboratory experiments and are commonly represented in the p-q space ("laboratory space") where p is the mean stress and q is the deviatoric stress. Mathematically, the three principal stresses and the p-q space are related as follow:

$$p = \frac{1}{3}J_1 = \frac{1}{3}(\sigma_1 + \sigma_2 + \sigma_3) \quad \text{..... (3)}$$
$$\Rightarrow p = \frac{1}{3}(S_V + S_{H\max} + S_{h\min}) - P_P$$

$$q = \sqrt{3J_{2D}} \Rightarrow$$
$$q^2 = \frac{1}{2}\left[\begin{array}{l}(S_V - S_{H\max})^2 + (S_{H\max} - S_{h\min})^2 \\ + (S_V - S_{h\min})^2\end{array}\right] \quad \text{..... (4)}$$

where P_P is the pore pressure and $\sigma = S - P_P$ is the effective stress. J_1 and J_{2D} are the first and the second invariant of the stress deviations tensor respectively. If the *in-situ* stress state in the reservoir is within the domain bounded by the failure envelope in p-q space, the formation is not likely to undergo deformation (Point I in Figure 2).

As reservoir depletion occurs, decreases in pore pressure as a result of production will increase the effective stresses within the reservoir. Once these increasing effective stresses reach a failure surface, deformation will occur. Deformation such as compaction and grain rearrangement (and eventually grain crushing and pore collapse) are the dominant deformation mode when the mean effective stresses are significantly higher than the deviatoric effective stresses. A corresponding decrease in both porosity and permeability[8] is expected. To represent these ductile yielding behaviors of rocks, end caps (or yield caps) are used. These end caps represent the locus of points with the same volumetric plastic strain and their shape depends on the material and the criterion model chosen[7]. The intersection of the yielding locus and the p-axis is defined as p_0 (also known as the preconsolidation pressure) and each end cap has its own unique p_0 that defines the hardening behavior of the rock sample. The value of p_0 can be determined easily from a series of hydrostatic compression tests in which porosity is measured as a function of confining pressure.

The equation of the yield loci shown in Figure 2a is derived based on the simple Cam-Clay model as given by Desai & Siriwardane[7]:

$$M^2 p^2 - M^2 p_0 p + q^2 = 0 \quad \text{..... (5)}$$

where M is known as the critical state line and can be expressed as $M=q/p$. In order to relate the critical state line with reservoir stress state, we need to express M in terms of the coefficient of friction, μ. The Mohr-Coulomb friction theory suggested that:

$$|\tau| = C_0 + \mu\sigma_n \quad \text{..... (6)}$$

where τ and σ_n can be expressed by:

$$\sigma_n = \frac{1}{2}(\sigma_1 + \sigma_3) + \frac{1}{2}(\sigma_1 - \sigma_3)\cos 2\beta \quad \text{..... (7)}$$

$$|\tau| = \frac{1}{2}(\sigma_1 - \sigma_3)\sin 2\beta \quad \text{..... (8)}$$

where sin2β and cos2β can be expressed in terms of μ^3 as

$$\sin 2\beta = \left(\mu^2 + 1\right)^{-½} \quad \text{and} \quad \cos 2\beta = -\mu\left(\mu^2 + 1\right)^{-½} \quad \text{..... (9)}$$

By combining Equation (6) to (10) and assuming the cohesion C_0 is negligible, we can express M in terms of μ as

$$M = \frac{6\mu}{3\sqrt{\mu^2 + 1} - \mu} \quad \text{..... (10)}$$

The critical state line is also known in cap models as the fixed yield cap surface that mark the critical state of stress at which shear failure will occur (Fig. 2a). Shear failure is discussed at greater length below.

During laboratory experiments, the changes in the hardening behavior of the rock sample result in a change in the size of the end cap. The end caps in Figure 2a mark the limit at which no inelastic compaction will occur if the stress state applied to the sample is within the end cap. However, if the sample is stressed beyond the end cap, inelastic compaction will occur and the sample will compact and become stronger. The "hardening" of the sample leads to an expansion of the end cap associated with the decrease in porosity.

While such a yielding surface analysis is widely used in engineering and laboratory experiments, it is obvious the changes in p and q through time may not readily applicable to a producing reservoir. Most *in-situ* measurements conducted in the reservoir involved the three principal stresses and pore pressure instead. As a result, we need to transform the yielding surface from the laboratory p-q space into the principal stresses-pore pressure space. To perform the transformation, we need to rearrange and express p and q as a function of the three principal stresses and pore pressure (i.e., S_{Hmax}, S_{hmin}, S_V, P_P, p_0 and M):

$$\begin{aligned} &9P_P{}^2 + \left(1 + \frac{9}{M^2}\right)\left(S_V{}^2 + S_{H\max}{}^2 + S_{h\min}{}^2\right) \\ &+ \left(2 - \frac{9}{M^2}\right)\left(S_V S_{H\max} + S_V S_{h\min} + S_{H\max} S_{h\min}\right) \quad \text{..... (11)} \\ &+ 9P_P p_0 - 3(2P_P + p_0)\left(S_V + S_{H\max} + S_{h\min}\right) \end{aligned}$$

The value of the vertical stress can be easily derived from density logs while M and p_0 can be determined from relatively simple laboratory experiments. For simplicity, we will limit ourselves to normal faulting regions where S_{hmin} is the least principal stress that can be obtained from LOT's and mini-fracs and, in a normal faulting regime, S_{Hmax} is somewhere between S_{hmin} and S_V. Because S_V remains constant with depletion and p_0 and M are material parameters, it is possible to project the ellipsoidal yielding surface onto the S_{hmin}-P_P domain (which we refer to as reservoir space in this paper). Thus, by combining the shear (Coulomb) failure envelope with the transformed end cap envelopes, a new composite diagram is created for analyzing the degree of compaction that is associated with reservoir depletion (Fig. 2b) and the likelihood that slip will be triggered on pre-existing faults. The evolution of the end caps of any given reservoir rock at different porosities can be used as an indicator of the deformation induced by the increase of the effective stresses due to the decrease in pore pressure during production.

The three stress paths on Fig. 2b represent hypothetical paths a reservoir may experience during depletion. Stress path 1 represents a relatively low $\Delta S_{hmin}/\Delta P_P$ ratio. If the reservoir depleted along this path, shear faulting is unlikely to occur but shear-enhanced compaction will take place and be the dominant mechanism of reservoir deformation with a change in porosity from ~40% to ~34%. Such a large change in porosity would likely result in significant compaction and permeability loss. If the stress path of the reservoir is steeper (stress path 2), the stress state in the reservoir will eventually hit the shear failure line and both compaction and normal faulting will be initiated (see discussions below). As depletion continues, the stress state in the reservoir will be controlled by the frictional strength resulting in stress path 3 on Figure 2b.

Deformation Analysis in Reservoir Space (DARS)

There are four essential steps to conduct a DARS analysis in a given reservoir. First, laboratory measurements of porosity and permeability reduction as a function of effective confining pressure are needed. These are straightforward measurements that can even be made on sidewall cores. An accurate and detail study on the rock behavior is essential since the accuracy of the DARS predictions are related to the quality of the laboratory experiments. Second, utilizing Cam-Clay model to extrapolate these data into p-q space (Fig. 2a) and then into reservoir space (Fig. 2b). Cam-Clay model was used in this study to bridge the laboratory space and the reservoir space because of its simplicity; however, other models can also be used. The different choice will only affect the detailed shape of the yield surfaces in both the laboratory space and the reservoir space. Third, the initial stress state in the reservoir must be estimated or measured. S_V can be determined from integration of density logs, S_{hmin} is determined from leak off tests (LOT) or mini-fracs and the initial pore pressure is usually known. It is also important to use LOT's carried out in the same unit as the pore pressure measurements. While it would be advantageous to know the magnitude of all three principal stresses, in the two cases presented below, the exact magnitude of S_{Hmax} is not critical. Finally, the reservoir stress path must be estimated, either using poroelastic theory (as discussed above) or empirical observations as will be done in the two cases considered below. When continuous stress measurements are not available, multi-well measurements can be used for estimating the stress path. However, it is important to examine if sub-compartments exist in the field. This can be determined easily by studying the pore pressure history of the selected wells. If the reservoir has no sub-compartment, the pore pressure measurements through time from all wells should be decreasing continuously at a given datum. In this case, stress measurements from different wells through production can be used for stress path estimation.

Gulf of Mexico Field X

Gulf of Mexico Field X is located on the continental shelf of the Gulf Coast basin off the Texas coast. It is one of the several fields along the Lower Miocene normal growth fault trend. The reservoir is trapped by fault, rolled-over anticline with sand expansion as a result of the growth fault and thinning from the crest to the anticline. The sand is deltaic and has a porosity ranging from 18 to 33%. The discovery well was drilled in 1980 and the field went into production in 1985 with an initial gas column of over 220 m and initial pressure of about 82 MPa.

Minifracs and LOT data were provided to constrain the magnitude of the S_{hmin} while drill-stem tests (DST's) and remote formation tests (RFT's) are available to constrain pore pressure. Pore pressure measurements from most wells in the region were compiled and corrected to a datum and a continuous decrease in P_P and the least principal stress can be observed (Fig. 3). This continuous trend of the pore pressure curve indicates that the reservoir is interconnected and sub-compartments are unlikely to be present. The evolution of the S_{hmin} and P_P is presented in Figure 4. As no information about the initial S_{hmin} is available, we projected the empirical stress path back to the original pore pressure and estimate the approximate magnitude of S_{hmin} at initial pore pressure. Notice that the empirical stress path in Field X is lower than the normal faulting line (i.e., a stable stress path), as a result, production seems to stabilize the reservoir with respect to normal faulting. In other words, the initial stress state was one in which normal faults were active, but depletion caused these faults to stabilize.

Laboratory experiments on seven samples collected from the reservoir formation from two different studies were used for determining the stress dependency of porosity and permeability (Fig. 5). The three circles with different shades are experiments conducted in one study while the squares and triangles are samples tested in another study. At about 50MPa, there is a marked change in the rate of porosity and permeability reduction. We term this a deformation threshold. Such changes are believed to be a result of a change in deformation mode from grain rearrangement to grain crushing and had been reported in other laboratory studies[8,9]. Figure 5c and 5d are normalized porosity and permeability changes with respect to confining pressure. Although the original porosity of all 7 samples are quite different, Figure 5c shows that their responses to increasing confining pressure in terms of porosity change are quite similar. Note that one of the studies (circles) did not load the sample beyond the deformation threshold.

Figure 6 demonstrates how such laboratory studies can be used in the DARS analyses. The porosity changes data are used due to the similarity among the compacting behavior of the samples. Figure 6a and b are porosity changes (or compaction) and porosity predicted from DARS based on the relationship shown in Figure 5c. Unlike Valhall, where production-induced normal faulting appears to occur as a result of high stress path, A=0.9[2], the relatively low stress path in GOM Field X implies that shear-enhanced compaction will be the dominating deformation mode and production-induced normal faulting is unlikely to occur. Note that the current stress condition in the reservoir is beyond the deformation threshold of the formation. It is therefore important to carefully examine how the sample deformed beyond the threshold in order to give a more accurate estimation of porosity change in the reservoir. Figure 6b demonstrate the predicted porosity from a typical sample of the producing reservoir (with an average initial porosity of 23%). The DARS analysis estimates an 11% of compaction in the formation while the porosity of the typical sand reduced from about 23% to 21%.

The relationship between porosity reduction and permeability reduction is summarized in Figure 8. The upper- and lower-bound are computed based on the results from the seven samples used in this study. The results from already published data (noted '+' in Fig. 7) are for deep-water turbidites in the Gulf of Mexico[10]. The two limits provide constraints on how porosity reduction is related to permeability reduction. This relationship is then used for predicting the change in permeability in the reservoir as a result of depletion-induced compaction (Figure 8). Figure 8 shows the predicted permeability of GOM Field X as a result of production-induced compaction based on the two limiting cases in Figure 7. The DARS analyses suggested that the change in permeability for Field X due to production-induced compaction is expected to be quite large: from ~225md to ~50-140md.

Conclusions

The DARS formalism provides a straightforward method to assess how a reservoir will deform with depletion and considers both compaction and induced faulting. To perform a DARS analysis, relatively simple laboratory experiments on how the porosity and permeability change with effective confining pressure are needed. Measurements of the changes in the horizontal stress and pore pressure within a reservoir are preferred over utilizing poroelastic theory. The advantage of using empirical stress paths is that assumptions about elastic moduli of the formation are not required. If such information is available, it is possible to predict the amount of compaction that is likely to occur in a depleting reservoir and whether normal faulting is likely to be induced during its producing lifetime.

Nomenclature

A = ratio of the change in horizontal stress to the change in pore pressure through time
ΔS_h = change in horizontal stress
ΔP_P = change in pore pressure
S_{Hmax} = maximum horizontal stress, MPa
S_{hmin} = minimum horizontal stress, MPa
S_v = vertical stress, MPa
P_P = pore pressure, MPa
μ = coefficient of friction
ν = Poisson's ratio
α = Biot's coefficient

K_b = bulk modulus of the bulk rock, GPa
K_g = bulk modulus of the mineral grains, GPa
p = mean stresses (in laboratory space), MPa
p_0 = preconsolidation pressure, MPa
q = deviatoric stresses (in laboratory space), MPa
J_1 = first invariant of the stress tensor
J_{2D} = second invariant of the stress deviation tensor
σ = effective stresses, MPa
M = critical state
τ = shear stresses, MPa
C_0 = cohesion, MPa
β = angle of internal friction

Acknowledgments

We thank BP-Amoco for providing the GOM Field X data used in this study. Financial support for this project was provided by the USGS (Contract No. 2BCZ-418) and the Stanford Rock and Borehole Geophysics project.

Reference

1. Segall, P. & Fitzgerald, S. D. 1996. "A note on induced stress changes in hydrocarbon and geothermal reservoirs". *Tectonophysics* **289**: 117-128.
2. Zoback, M.D. & Zinke, J.C., 2002. "Production-induced normal faulting in the Valhall and Ekofisk oil fields". *Pure and Applied Geophysics*, **159**, 403-420.
3. Jaeger, J.C. & Cook, N.G.W. 1969, *Fundamentals of Rock Mechanics*. Methuen and Co. Ltd.: London, 515p.
4. Byerlee, J.D. 1978. *Friction of Rock, Pure and Applied Geophysics* **116**: 615-626.
5. Zoback, M.D. & Healy, J.H., 1984. "Friction, faulting and '*in situ*' stress". *Annales Geophsicae*, **2**, 689-698.
6. Townend, J. & Zoback, M.D. 2000. "How faulting keeps the crust strong". *Geology* **28**: 399-402.
7. Desai, C.S. & Siriwardane, H.J. 1984. *Constitutive Laws for Engineering Materials, with Emphasis on Geologic Materials*. Prentice-Hall: Englewood Cliffs, N.J., 468p.
8. Zhu, W. & Wong, T.F., 1997. "The transition from brittle faulting to cataclastic flow: permeability evolution". *J. Geophys. Res*., **102**, 3027-3041.
9. Wong, T.F., David, C., Zhu, W. 1997. "The transition from brittle faulting to cataclastic flow in porous sandstones: mechanical deformation". *J. Geophys. Res*., **102**, 3009-3025.
10. Ostermeier, R. M., 2001, "Compaction effects on porosity and permeability: deepwater Gulf of Mexico turbidites" *JPT. Journal of Petroleum Technology*, **Feb. 2001**, p. 68-74.
11. Salz, L.B. 1977. "Relationship between fracture propagation pressure and pore pressure". *SPE 6870, 52nd Annual Conf., Denver, Colorado, 9-12 October 1977*.
12. Whitehead, W.S., Hunt, E.R. and Holditch, S.A. 1987. "The effects of lithology and reservoir pressure on the in-situ stresses in the Waskom (Travis Peak) Field". *Society of Petroleum Engineering*, Paper 16403
13. Addis, M.A. 1997. "Reservoir depletion and its effect on wellbore stability evaluation". *International Journal of Rock Mechanics and Mining Sciences*, **34**, 3-4, Paper 4.
14. Finkbeiner, T., 1998. "In-situ stress, pore pressure and hydrocarbon migration and accumulation in sedimentary basins". *PhD thesis, Department of Geophysics, Stanford University, CA*. 193pp.

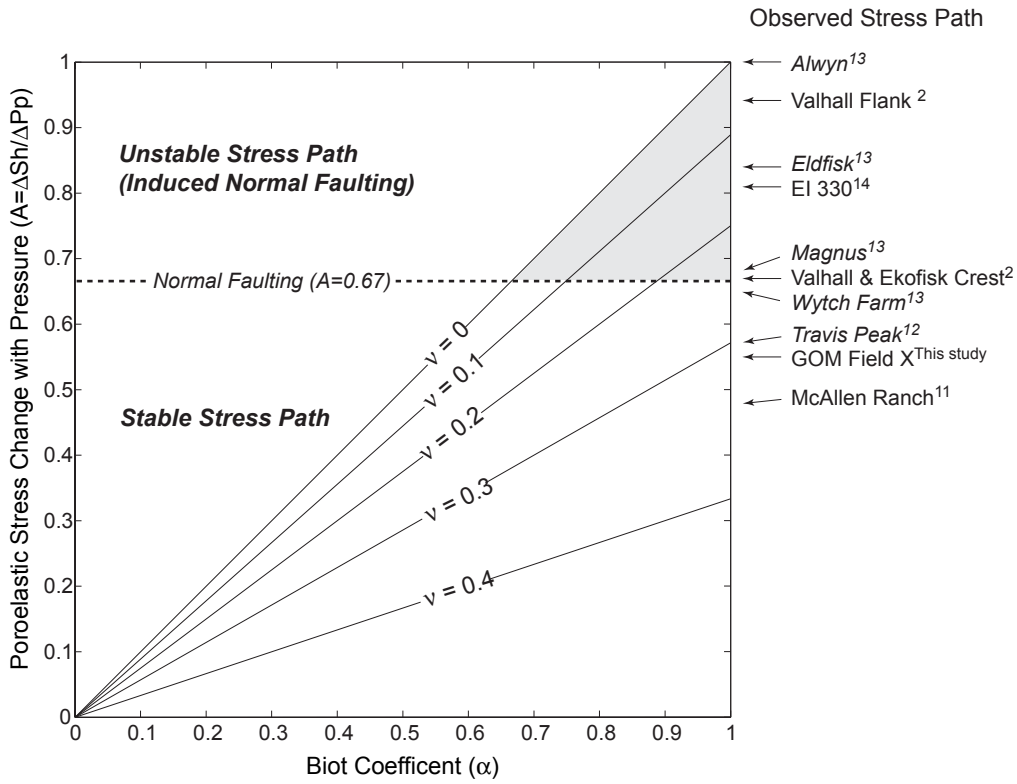

Figure 1: Variation of stress change with pressure as a function of Biot coefficient, α, and Poisson's ratio, ν. The normal faulting line represents *A* = 0.67 (see text). The gray area represents the possible combination of α and ν such that stress path leads to production-induced normal faulting. Observed stress paths in different reservoirs are shown on the right hand side of the diagram. For the fields listed in *italics*, it is not clear whether the reported 'stress path' indicates a change of stress with depletion or variation of stress with pore pressure in different part of the fields.

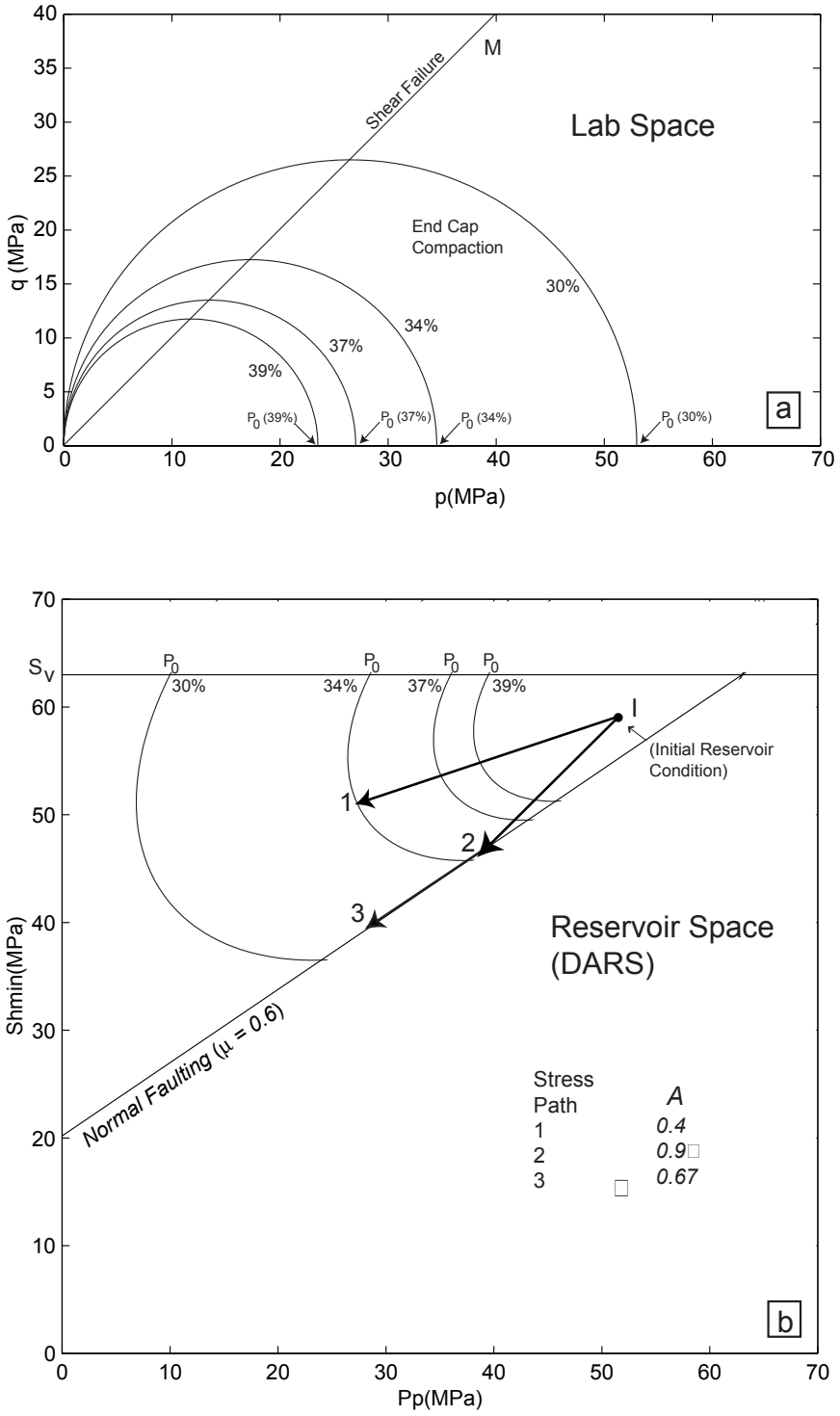

Figure 2: The transformation of end caps from laboratory space (p-q) into reservoir space (S_{hmin}-P_P) based on the Cam-Clay model. (a) Schematic diagram in laboratory space showing the changes in porosity of a rock sample as a result of changes in pressure where p is the mean stress and q is the deviatoric stress. As pressure increases, the porosity of the rock sample decreases. This behavior is reflected by the increase of the size of the end cap. The end cap represents the limit at which inelastic compaction will occur while M marks the critical state line. The critical state line is also known as the fixed end cap in some contexts. Curves above the shear failure line only presented as a completeness of the yielding loci. (b) The transformed end caps in reservoir space. Stress paths 1, 2 and 3 are possible stress paths that a depleting reservoir may follow. If the stress path is steeper than the critical value of 0.67, the producing reservoir will eventually reaches the normal faulting stress states as in stress path 2. If depletion continues to occur, the reservoir will deform following stress path 3 and induced normal faulting will continue. However, when *A* is smaller than 0.67, normal faulting is unlikely to occur. Indeed, the reservoir will become more stable from faulting. Stress path 1 shows such scenario and notice that compaction will still occur as production continues.

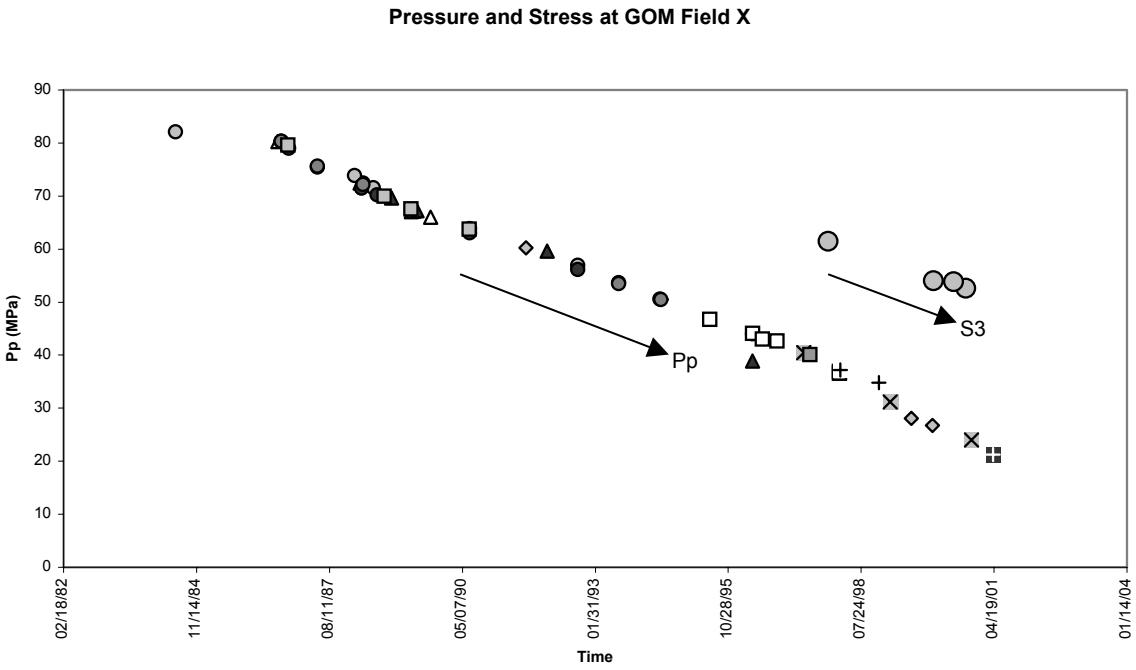

Figure 3: Pore pressure history of the GOM Field X. Different symbols represent measurements made in different wells. The magnitude of the pore pressure is then adjusted to the datum. Notice that the continuous decline of pore pressure measurement from different well implies that there is no sub-compartmentalization within the reservoir.

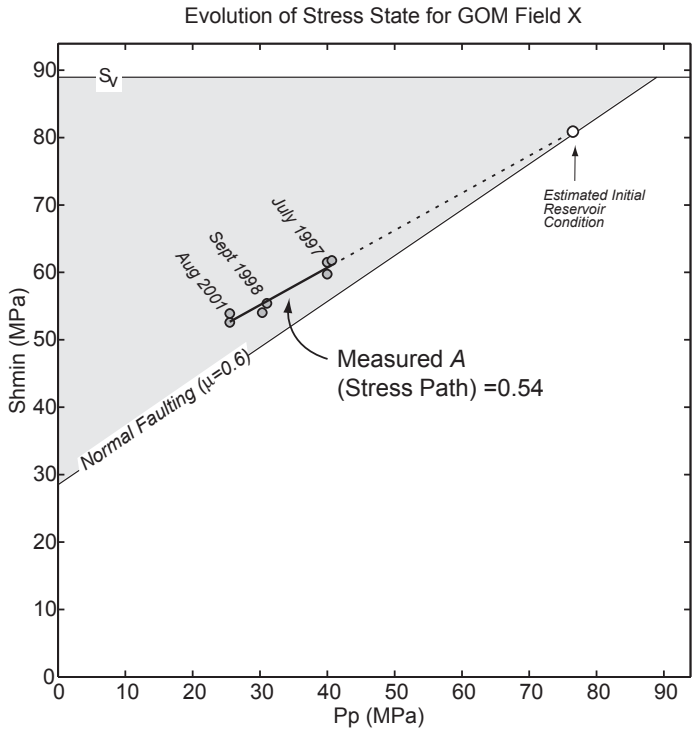

Figure 4: Stress measurements throughout the lifetime of the reservoir. Most measurements are recorded in the 1990s while none is made during the early stage of the production. Stress path is estimated based on the limited data points obtained. The initial reservoir condition is estimated based on the stress path presented. It is obvious that the reservoir initially is in a state of faulting equilibrium and moved away from failure as production continues. Production, in this case, is not likely to induce normal faulting within the reservoir sand.

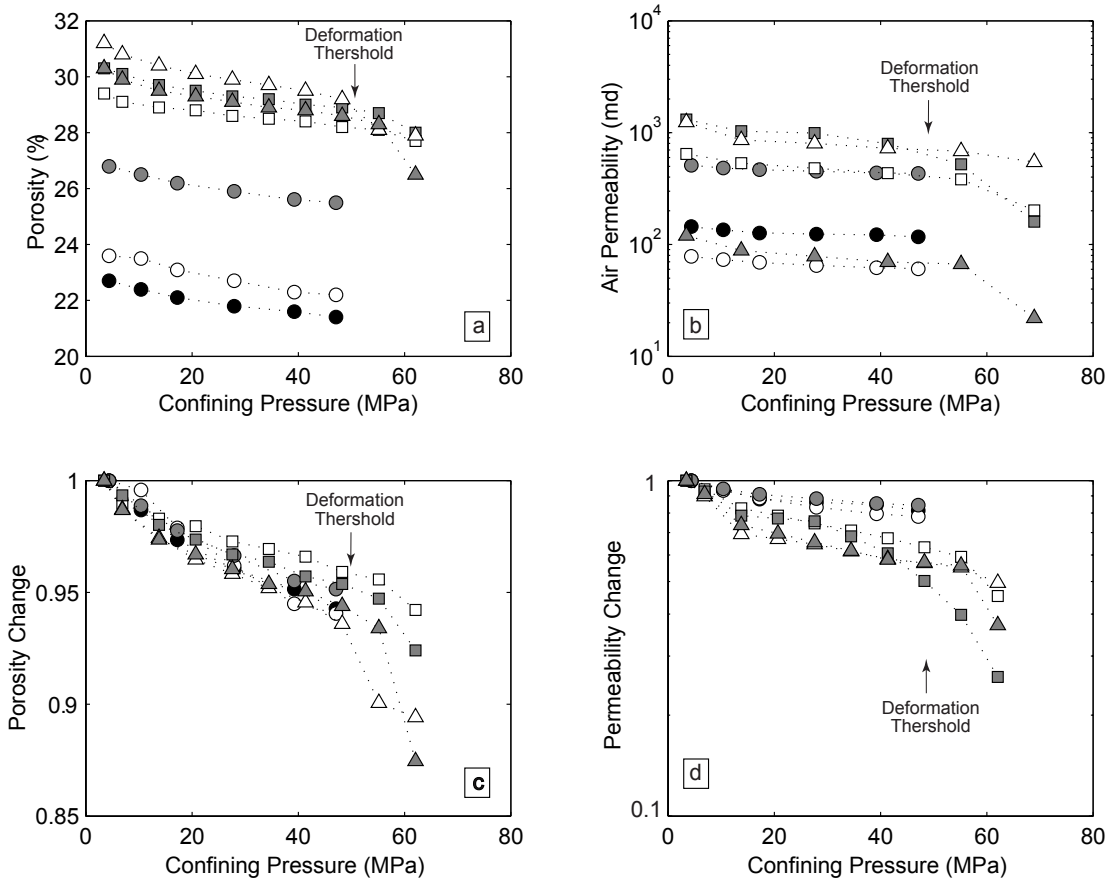

Figure 5: Stress dependence of porosity and permeability for seven samples collected from the producing formation in Field X. The three circles with different shades are experiments conducted in one study while the squares and triangles are sample tested in another study. There is a marked change in the rate of porosity and permeability reduction at about 50 MPa. Such change is termed deformation threshold in this study. Note that these three samples are loaded to the deformation threshold. (a) & (b) are the porosity and permeability measurements as a function of confining pressure. (c) & (d) are the porosity and permeability changes with respect to confining pressure. Note that the porosity changes for all samples are very similar even though the initial porosities are quite different.

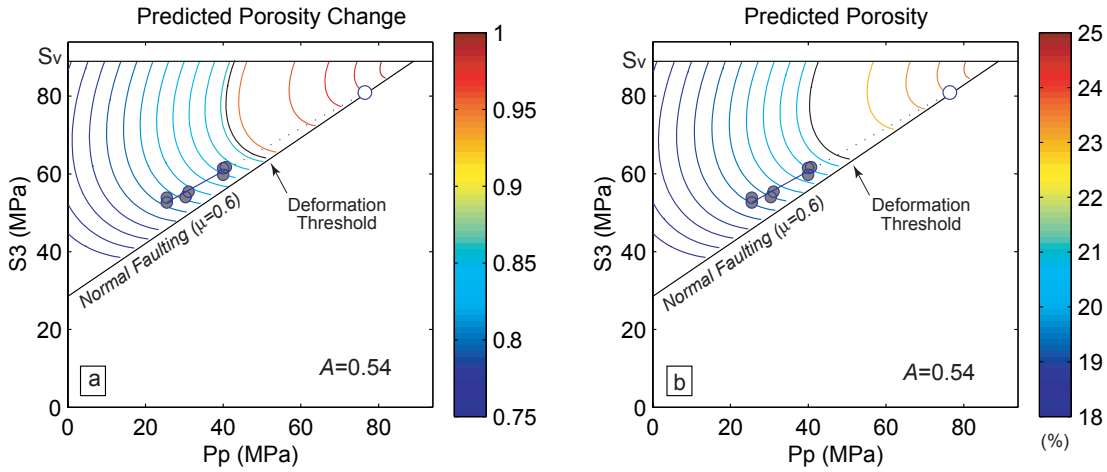

Figure 6: DARS predictions on porosity change (or compaction) and porosity for Field X based on laboratory experiments (Fig. 5). The data points represent the in-situ stress measurements (as in Fig. 4). The black contour corresponds to the deformation threshold from Figure 5.

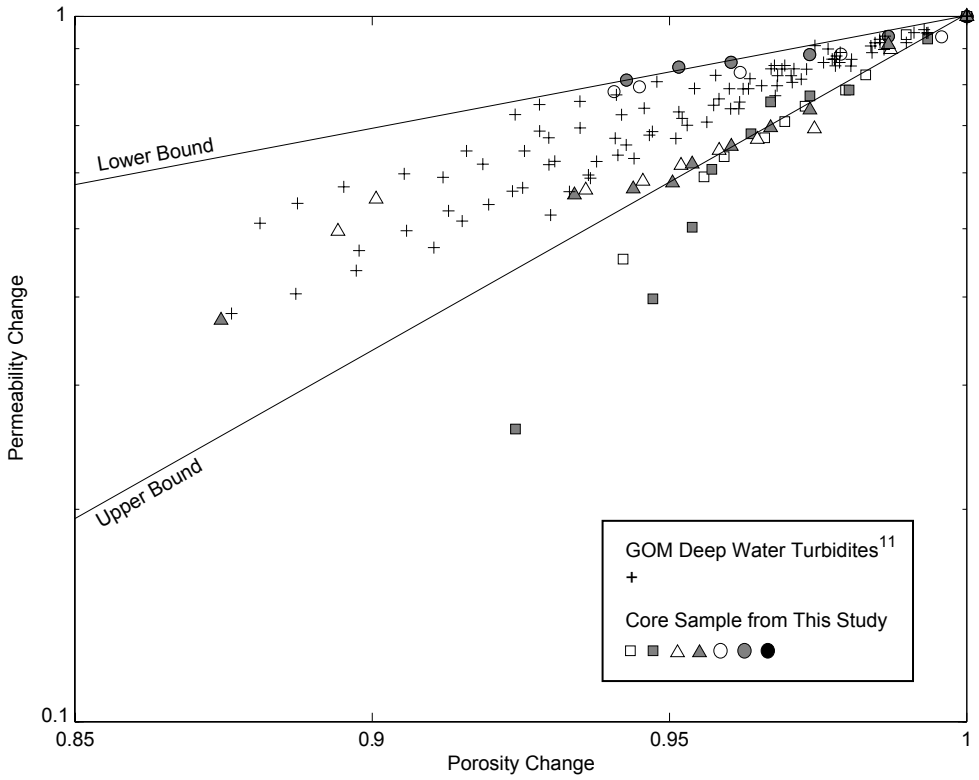

Figure 7: Comparison of permeability change as a function of porosity change from this study and reported values from Ostermeier[11]. The two limits are estimated based on the results from the seven samples used in this study. Note almost all of the data collected from this study and the Ostermeier study fall between the lower and the upper bound suggesting a relatively consistent relationship between permeability change and porosity change for Gulf of Mexico turbidite sands.

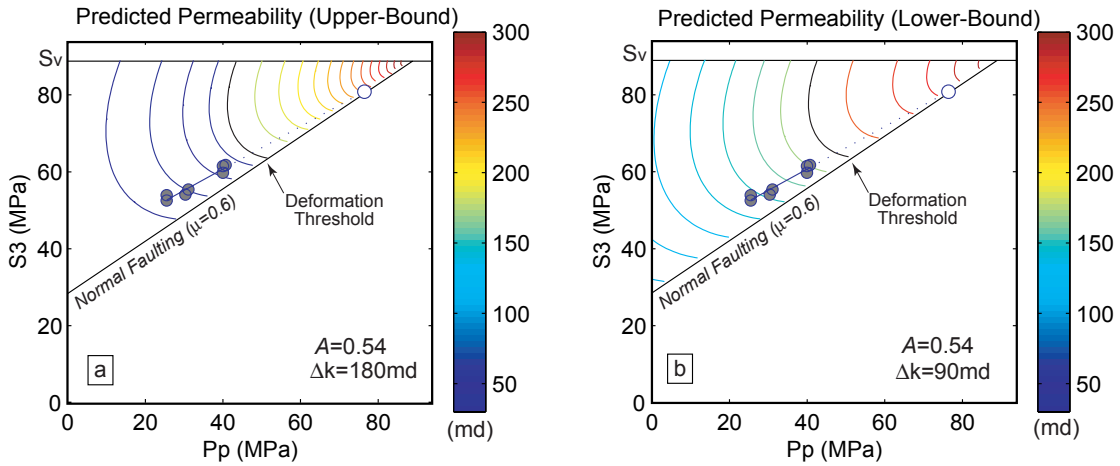

Figure 8: Predicted permeability loss in GOM Field X based on the relationship of porosity reduction and permeability reduction as described in Figure 7. The range of permeability reduction as a result of compaction is between 90md and 180md.